Reconstruction of Pulse Wave and Respiration From Wrist Accelerometer During Sleep

Article *in* IEEE transactions on bio-medical engineering · August 2021

DOI: 10.1109/TBME.2021.3107978

7 authors, including:

Johannes Zschocke
Martin Luther University Halle-Wittenberg
7 PUBLICATIONS **22** CITATIONS
SEE PROFILE

Martin Glos
Charité Universitätsmedizin Berlin
166 PUBLICATIONS **1,463** CITATIONS
SEE PROFILE

Thomas Penzel
Charité Universitätsmedizin Berlin
1,139 PUBLICATIONS **19,210** CITATIONS
SEE PROFILE

Reconstruction of Pulse Wave and Respiration from Wrist Accelerometer During Sleep

Johannes Zschocke, Julian Leube, Martin Glos, Oxana Semyachkina-Glushkovskaya, Thomas Penzel, Ronny P. Bartsch, and Jan W. Kantelhardt

***Abstract*— *Objective:* Nocturnal recordings of heart rate and respiratory rate usually require several separate sensors or electrodes attached to different body parts – a disadvantage for at-home screening tests and for large cohort studies. In this paper, we demonstrate that a state-of-the-art accelerometer placed at subjects' wrists can be used to derive reliable signal reconstructions of heartbeat (pulse wave intervals) and respiration during sleep. *Methods:* Based on 226 full-night recordings, we evaluate the performance of our signal reconstruction methodology with respect to polysomnography. We use a phase synchronization analysis metrics that considers individual heartbeats or breaths. *Results:* The quantitative comparison reveals that pulse-wave signal reconstructions are generally better than respiratory signal reconstructions. The best quality is achieved during deep sleep, followed by light sleep N2 and REM sleep. In addition, a suggested internal evaluation of multiple derived reconstructions can be used to identify time periods with highly reliable signals, particularly for pulse waves. Furthermore, we find that pulse-wave reconstructions are hardly affected by apnea and hypopnea events. *Conclusion:* During sleep, pulse wave and respiration signals can simultaneously be reconstructed from the same accelerometer recording at the wrist without the need for additional sensors. Reliability can be increased by internal evaluation if the reconstructed signals are not needed for the whole sleep duration. *Significance:* The presented methodology can help to determine sleep characteristics and improve diagnostics and treatment of sleep disorders in the subjects' normal sleep environment.**

Submitted: 26.04.2021. This work was supported in part by German Israeli Foundation (GIF) Grant No I-1372-303.7/2016, by the German National Cohort (GNC) (www.nako.de), funded by the Federal Ministry of Education and Research (BMBF) and the Helmholtz Association, and by the Russian Federation Government Grant No 075-15-2019-1885.

J. Zschocke is with the Institute of Medical Epidemiology, Biometrics and Informatics (IMEBI) Interdisciplinary Center for Health Sciences and the Institute of Physics, Martin-Luther University Halle-Wittenberg, Halle (Saale), Germany (johannes.zschocke@physik.uni-halle.de).

L. Leube is with the Department of Nuclear Medicine, University of Würzburg, Würzburg, Germany, and was with the Institute of Physics, Martin-Luther University Halle-Wittenberg, Halle (Saale), Germany (leube_j@ukw.de).

M. Glos is with the Interdisciplinary Sleep Medicine Center, Charité - Universitätsmedizin Berlin, Berlin, Germany (martin.glos@charite.de).

O. Semyachkina-Glushkovskaya is with the Saratov State University, Saratov, Russia (glushkovskaya@mail.ru).

T. Penzel is with the Interdisciplinary Sleep Medicine Center, Charité - Universitätsmedizin Berlin, Berlin, Germany and the Saratov State University, Saratov, Russia (thomas.penzel@charite.de).

R. P. Bartsch is with the Department of Physics, Bar-Ilan University, Ramat Gan, Israel (bartsch.ronny@gmail.com).

J. W. Kantelhardt is with the Institute of Physics, Martin-Luther University Halle-Wittenberg, Halle (Saale), Germany (jan.kantelhardt@physik.uni-halle.de).

***Index Terms*— Accelerometers, Biomedical monitoring, Signal reconstruction, Pulse waves, Respiration, Time series analysis, Sleep stages, Sleep apnea**

I. Introduction

SLEEP disturbances are associated with impaired health and well-being, reduced performance and higher risk of adverse events and accidents [1]–[5]. Specifically, there is evidence of a link between insomnia, sleep apnea, or unusually short or long total sleep durations and risk factors for major cardiovascular diseases, morbidity, and mortality [6]–[8]. However, the explanatory value of many such studies is limited because of restrictions in the study designs, or limitations in the methods used for the assessment. Therefore, it is premature to infer causal relationships from the current body of literature. Additional large prospective studies thus have to address sleep characteristics as possible determinants of personal health in more differentiated ways in large subject populations [9].

Although cardiorespiratory polysomnography (PSG) has been regarded as the gold standard in sleep medicine since 1968 [10], [11], its intricacy and costs disallow studying very large subject populations. Beyond that, PSG may produce first-night effects and may lead to a selection bias [12]–[14]. As an alternative to PSG, movement-based methods, such as actigraphy (or accelerometry), have been established since 1974 [15], [16]. Advantages of accelerometry over PSG are described as lower costs, higher availability, easy recording of multiple nights, and lower influence on natural sleep [17]–[20]. However, the full potential of modern accelerometers with long-term three-axis recordings at sampling rates above 100 Hz and acceleration resolutions of just a few milli-g[1], i.e., a few thousandth of the gravitational acceleration on earth, still needs to be explored [9].

In this paper we describe and evaluate procedures for deriving reconstructions of cardiac dynamics (through the reconstruction of the pulse wave signal) and respiratory activity from wrist accelerometer data. While we have already introduced the overall methodological approaches in two previous publications [21], [22], this study is the first systematic evaluation that takes into account sleep architecture, i.e., different sleep stages and sleep disorders such as sleep apnea. Based on 226 full-night recordings from typical patients of a clinical sleep laboratory, we characterize the reliability of

[1]In this paper we use g as gravitational acceleration of 9.81 m/s^2.

our pulse wave signal reconstructions and respiration signal reconstructions by means of a phase synchronization analysis that quantifies the similarity of the reconstructed data with reference heartbeat (RR) and respiratory flow data as recorded by PSG.

The paper is organized as follows. In Section II we describe our study population, the data recordings, and the data preprocessing, followed by our techniques for calculating pulse wave reconstructions and respiratory reconstructions from the same wrist acceleration time series. We also describe the phase synchronization analysis technique we use to quantify the similarity of the reconstructed signals with the recorded reference signals as well as our surrogate data analysis for statistical testing. The results are presented in Section III, including an additional suggestion for internal evaluation of the reconstructed data to identify temporal periods and channels with particularly reliable data. The paper concludes with discussion and outlook presented in Section IV. Some technical details regarding the synchronization of time series data from different recording devices and reconstruction techniques are reported in the supplementary material to facilitate other implementations of our ideas.

II. Data and methods

A. Data

We analyzed single night data from 226 subjects recorded in clinical sleep laboratories at the Charité-Universitätsmedizin Berlin, Germany, between April 2017 and March 2019. The study was approved by the ethics committee of the Charité-Universitätsmedizin Berlin and registered at the German Clinical Trial Register (DRKS) with ID DRKS00016908. All enrolled subjects gave written informed consent prior to the study. During their first diagnostic night at the sleep laboratory, all subjects wore a SOMNOwatch™ plus device (SOMNOmedics, Randersacker, Germany), recording simultaneously 3d wrist acceleration of the nondominant arm at 128 Hz sampling rate as well as one channel electrocardiogram (ECG) at 256 Hz. For this purpose, a thin cable leading to three electrodes placed below each collarbone and above the fifth intercostal space of the left side of the body is attached to the watch-like device worn at the wrist of the non-dominant hand. A picture of the device is shown in the online supplementary material. Furthermore, full polysomnography (PSG) (including electroencephalography (EEG), electrooculography (EOG), electromyography (EMG), ECG, photoplethysmogram (PPG), oxygen saturation, respiratory effort, etc.) was recorded using either an ALICE (Philips, Amsterdam, Netherlands), an Embla® (Natus, Pleasanton, USA), or a SOMNOscreen™ PSG system (SOMNOmedics, Randersacker, Germany).

Since accelerometry was recorded only by SOMNOwatch™, while sleep stages and reference respiratory activity were available only from the PSG systems, as initial step we had to establish synchronization between the recording devices. This turned out more intricate than expected because the clocks of the devices drifted with respect to each other by several seconds throughout the night, and brief interruptions occurred in the PSG recordings. However, since all devices recorded ECGs, a one-to-one matching of the R-peak positions was used for establishing synchronization, see the supplementary material for details. Due to insufficient ECG quality mainly in the PSG systems' data, this procedure was unsuccessful for 105 subjects (i.e., recording nights), reducing the number of available data correspondingly. Another 108 subjects had to be excluded because of noisy or corrupt respiration recordings. Therefore, only 226 out of the original 439 data sets were available for analysis. To show that no bias was introduced this way, we have compared many clinical and sleep-related parameters for the 226 data sets we used and the 213 we excluded, see Table **??** in the supplementary material. The final used data set consists of single-night recordings of 109 female and 117 male participants with body mass index 27.9 ± 5.7 [17.0, 51.5] kg/m^2, age 48.6 ± 13.9 [18.1, 78.4] years, and time in bed 7.6 ± 0.8 [5.4, 10.2] hours (mean $\pm$ standard deviation [minimum, maximum]). Each measurement was cropped to only contain data between the 'lights off' and 'lights on' time stamps, indicating beginning and end of the sleep opportunity period, respectively.

B. Overview of Previous Works for Reconstructing Cardiac and Respiratory Activity from Acceleration Sensor Data

In seismocardiography, acceleration sensors placed on the chest wall measure the vibrations caused by heartbeats [23]. In recent years, this technique became more relevant due to better accelerometers [24], [25]; it has also been used to assess respiratory activity [26], [27]. Besides respiration (< 1 Hz), low frequency (0.6 to 5 Hz) chest wall motions caused by heart muscle contraction and high frequency (> 5 Hz) chest wall vibrations related with acoustic waves of the valve closing are measured [26], [28]. In ballistocardiography whole body motions (or vibrations) caused by the heart (and respiration) are measured. Sensors are commonly placed on the bed [24], [29], [30], a recliner chair [31] or a vehicle seat [32]. Accelerometer-based methods for measuring breathing-related movements have been roughly validated [26], but mainly accelerometers and gyroscopes positioned over the diaphragm [33], the chest wall [34] or the forehead [35], [36] have been considered. The latter two publications also used wrist accelerometry to estimate heart rates and respiratory rates. However, they focused on average rates in 20 s intervals as determined via spectral analysis, not trying to identify individual heartbeats or breaths, and were limited to 32 h of sleep data from three subjects plus daytime data. Another paper reported that heart rate can most reliably be estimated via accelerometry, if the sensor is attached to the subjects' upper forearm or the subjects' belly [37]. A recent study [38] also considered a sensor placement on the upper arm, together with a sensor at the foot and finger plethysmography, studying data recorded during standing and hemodynamic interventions.

C. Reconstruction of Pulse Wave Signals from Wrist Accelerometer Data

Pulse waves transversing the wrist initiate damped vibrations of the tissue at frequencies around 8 Hz [9], [42]. These

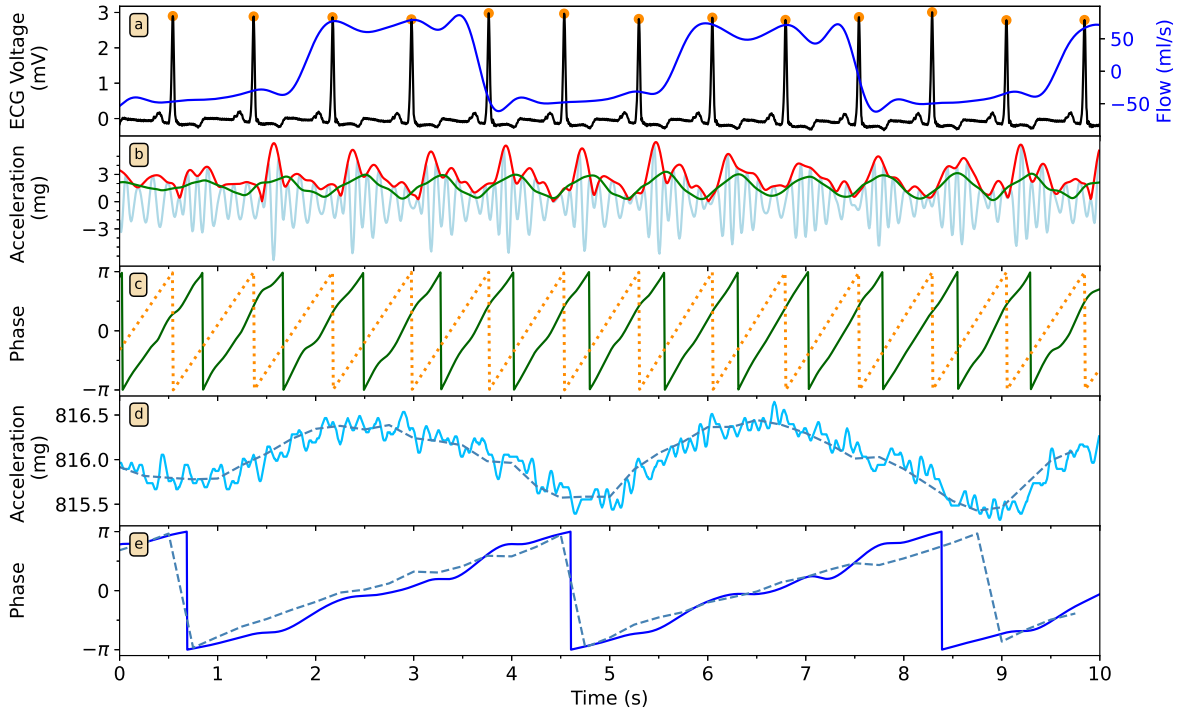

Fig. 1. **Signal processing procedure** as demonstrated for an epoch of 10 seconds of data for a typical subject. (a) In the ECG signal (black curve) recorded by the SOMNOwatch™ device, R-peaks are marked by orange dots. The respiration flow signal recorded simultaneously by the PSG system is shown in blue. (b) By passing through the wrist, pulse pressure waves cause tiny high frequency vibrations that can be measured by an accelerometer. The light blue curve depicts these vibrations for the $\boldsymbol{y}$ axis after 5-14 Hz bandpass filtering. The envelope of this signal (red curve), as derived by the analytic signal approach [39], [40], shows one high peak and several smaller peaks after each heartbeat, representing the main pulse pressure wave as well as its reflections. These reflections are erased by a smoothing procedure, which results in our pulse wave reconstruction (green curve). (c) The instantaneous phase of the oscillating pulse wave reconstruction (green curve) is plotted together with the ECG phase (dotted orange curve) that is obtained by linear interpolation between the R-peaks ("Poincaré method" [41]). (d) The respiratory activity signal is derived from the same $\boldsymbol{y}$ axis wrist accelerometer recording as used in (b) by applying a one-second moving average filter (light blue curve). The respiration reconstruction (dashed blue curve) is obtained by further smoothing and down sampling. Panel (e) shows the instantaneous respiratory phases derived from the flow signal (from panel (a), solid blue curve) and from the processed accelerometer signal (from panel (d), dashed blue curve).

fast oscillations are slightly but sufficiently above the detection threshold of the wrist accelerometer (at $\approx 3\mathrm{mg} \approx 0.003\mathrm{m/s}^2$; the accelerometer digitizes at a resolution of 12 bit for the range $-6g$ to $+6g$)[2]. In the field of radio telecommunication, the high frequency tissue vibration would represent a carrier frequency, which is amplitude-modulated by the pulse wave. Therefore, after bandpass filtering in the range of 5 to 14 Hz, the registered acceleration signal appears like an amplitude modulated carrier frequency (light blue curve in Fig. 1 (b)). The instantaneous amplitudes of the carrier are obtained by calculating its Hilbert transform, constructing the analytic signal [39], [40] and taking the absolute value (red curve in Fig. 1(b)). This envelope signal is modulated by systolic and diastolic pressure changes as well as reflections of the pulse wave coming back from the hand. After applying a suitable smoothing procedure (see [21] and supplementary material), we obtain a reconstruction for the systolic pulse wave (green curve in Fig. 1 (b)).

We apply the same signal processing procedure to all three recording axes (x, y, z) of the accelerometer to obtain the acceleration-based pulse wave signal reconstructions A_x^{PW}, A_y^{PW}, and A_z^{PW}. To take into account that combinations of the three acceleration axes could improve our results, we derive two additional pulse wave signal reconstructions A_ϕ^{PW} and A_θ^{PW} for the wrist rotation angles ϕ, rotation around the lower arm, and θ, turning angle with respect to the elbow (see supplementary material for more details).

[2]Corresponding to the technical details of a SOMNOwatch™.

D. Reconstruction of Respiration Signals from Wrist Accelerometer Data

Respiratory activity causes tiny periodic turns of the wrist, which can be detected via high-resolution accelerometer recordings [9], [22], [42], because the projection of the gravitational (vertical) direction on the recording axes changes periodically with the breathing cycle. Since modulations of the acceleration signal caused by respiratory activity are slower compared to pulse wave modulations, a moving average over intervals of one second is applied to the raw acceleration data for preprocessing (Fig. 1 (d) (light blue curve)), followed by downsampling to 4 Hz (Fig. 1 (d) (blue dotted curve)). The rotational angles ϕ and θ are also derived. Further smoothing procedures lead to the respiration signal reconstructions A_x^{RESP}, A_y^{RESP}, A_z^{RESP}, A_ϕ^{RESP}, and A_θ^{RESP} (see supplementary material for more details).

E. Comparison between Reconstructed Signals and Reference Signals

We evaluate the quality of the five pulse wave signal reconstructions and the five respiration signal reconstructions by systematically comparing them to the ECG and respiratory flow signal, respectively. To this end, we need to take into account that there is a small variable time delay between the contraction of the ventricular muscles (as registered by the R-peak in the ECG) and the pulse wave measured at the wrist. This time delay corresponds to the pulse transit time and is the reason for the few hundred milliseconds long shift between R-peaks in the ECG and the pulse wave signal reconstructions (compare R-peak positions and maxima of A_y^{PW} in Fig. 1 (a) (red curve) and (b) (black curve) and the phase shift in (c)). In addition, respiratory activity derived from wrist motion is also likely to be phase shifted with respect to the respiratory flow, because variations of the wrist angles can either be in synchrony with the maxima or the minima of the lung volume. Hence, the quality of the signal reconstructions can be best evaluated by studying the *stability* of the time or phase delays or differences between reconstructions and their corresponding reference signals. Looking at phases instead of the signals themselves has the additional advantage of independence from the signals' amplitude, which is likely to fluctuate throughout the night due to different arm and wrist positions as well as varying positions of the recording device at the wrist. In addition, a comparison based on phases takes into account the full information in the signals' cycles and not just one data point from each cycle as for an event synchronization [43] or coordination [44] approach. This leads to more reliable statistics.

Instantaneous phases of the signal reconstruction have been obtained by means of a Hilbert transform and the analytic signal approach [39], [40] (see supplementary material for more details) and are shown in Fig. 1 (c) and (e) for pulse waves and respiratory activity, respectively. In order to derive an instantaneous phase from the ECG, we have performed a linear interpolation between the R-peaks ("Poincaré method" [41]). The R-peak-derived reference phase signal φ^{ECG} has thus sawtooth shape with jumps from $+\pi$ to $-\pi$ at the time positions of the R-peaks (orange dotted curve in Fig. 1 (c)). This signal is similar to the phase signal φ_y^{PW} derived from the reconstruction A_y^{PW} (green curve in Fig. 1 (c)), however, φ_y^{PW} does not have a constant slope from $-\pi$ to $+\pi$ and the phase jumps from $+\pi$ to $-\pi$ occur at shifted temporal positions relative to φ^{ECG} (due to the pulse transit time).

The temporal stability of a phase shift is quantified by phase synchronization indices (PSIs) [41]. A particular PSI can be calculated from pairs of phase signals, e.g., φ_y^{PW} and φ^{ECG}, by averaging complex exponentials of the phase difference over time epochs of duration T and taking the absolute value of the complex result [45],

$$\gamma_y^{PW}(t_0) = \left| \frac{1}{T} \int_{t_0}^{t_0+T} \exp[i\varphi_y^{PW}(t) - i\varphi^{ECG}(t)]\, dt \right|. \quad (1)$$

Here, i denotes the imaginary unit, and the integration turns into a sum for time series with a specific sampling rate. Equation (1) further shows that the PSI γ is not affected by a constant phase shift $\Delta\varphi$ since the exponential of an imaginary constant, $\exp(i\Delta\varphi)$, has an absolute value of one. Choosing time windows of $T = 30$ seconds duration, we obtain PSI values γ^{PW} for each epoch of 30 seconds and each of the five acceleration-derived pulse wave reconstructions, A_x^{PW}, A_y^{PW}, A_z^{PW}, A_ϕ^{PW}, and A_θ^{PW}.

The same approach is used for comparing the acceleration-derived respiratory reconstructions A_x^{RESP}, A_y^{RESP}, A_z^{RESP}, A_ϕ^{RESP}, and A_θ^{RESP} to the respiratory flow signal (Fig. 1 (a) (blue curve)). Fig. 1 (e) shows an example for the instantaneous respiratory phases φ^{FLOW} derived from the flow signal (solid blue curve) and the processed y axis accelerometer signal φ_y^{RESP} (dashed blue curve). We refer to the supplementary material for more details on reconstruction and phase computation.

F. Surrogate Data Testing

In order to probe the significance of our PSI results, we have performed two types of surrogate data tests. In the first test, the reference phases φ^{ECG} and φ^{FLOW} are replaced by surrogate phases created by inverting the time direction of the corresponding ECG and flow recordings. The results will show the level of PSI for unsynchronized data, i.e., the lower limit for relevant PSI values.

In the second surrogate test, we have replaced the reconstructed phases by phases φ^{PPG} derived from the PSGs PPG measured at the finger tips for a subgroup of 134 subjects. Since the PPG is assumed to represent the real pulse wave activity, this approach will yield an upper limit for PSI values, i.e., the PSI values that could be expected for optimal pulse wave reconstructions. Instantaneous pulse wave phases are derived from the PPG by the same filtering and smoothing procedure as was used for the acceleration-based pulse wave reconstructions.

III. Results

A. Time-Dependent and Average Phase Synchronization Index

Fig. 2 shows examples of PSI results for full nocturnal measurements of two subjects. For each epoch of 30 seconds, the quality of pulse wave reconstructions and respiratory reconstructions is indicated by γ_j^{PW} (Fig. 2 (orange curves)) and γ_j^{RESP} (Fig. 2 (purple curves)), considering different accelerometer axes and angles $j = x, y, z, \theta$ for the reconstructions. While reconstruction of pulse wave signals works very well, as indicated by γ_j^{PW} values close to one (i.e., perfect phase synchronization), respiratory reconstructions exhibit episodes of acceptable ($\gamma_j^{RESP} \geq 0.5$) as well as non-acceptable ($\gamma_j^{RESP} < 0.5$) quality. For example, for the time window from 3 to 5 h after lights-off in Fig. 2 (a), (b) and for long periods of the time in Fig. 2 (d) the respiratory signal can not be sufficiently reconstructed. Sometimes the reconstruction from one axis is clearly superior to the reconstruction from another axis (cp. much larger values of γ_x^{PW} in Fig. 2 (a) than γ_z^{PW} in (b) at around 7 h after lights-off).

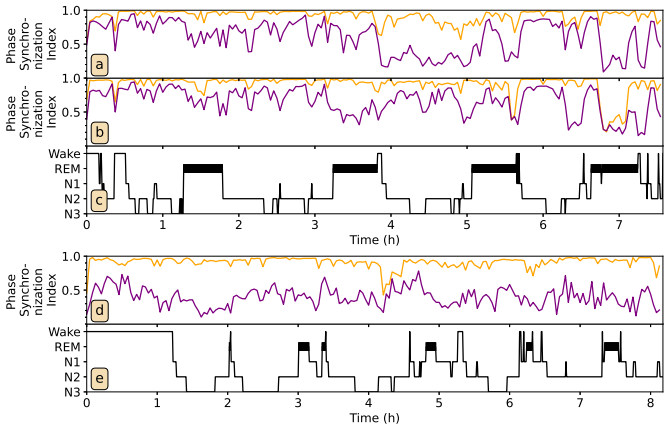

Fig. 2. **Phase synchronization indices (PSIs) for whole-night recordings** of two subjects. (a-c) For the first subject, PSIs of two pulse wave reconstructions, (a) $\gamma_{\boldsymbol{x}}^{\boldsymbol{PW}}$ and (b) $\gamma_{\boldsymbol{z}}^{\boldsymbol{PW}}$ (orange curves) show good reconstruction quality except for around 7 h after lights-off for $\gamma_{\boldsymbol{z}}^{\boldsymbol{PW}}$. The quality of the respiratory reconstructions, (a) $\gamma_{\boldsymbol{x}}^{\boldsymbol{RESP}}$, (b) $\gamma_{\boldsymbol{z}}^{\boldsymbol{RESP}}$ (purple curves) is mixed, since PSI curves frequently drop to low values in the second half of the night. A complementary behavior of $\gamma_{\boldsymbol{x}}^{\boldsymbol{RESP}}$ and $\gamma_{\boldsymbol{z}}^{\boldsymbol{RESP}}$ in the period between 3 h and 5 h after lights-off (i.e., low values of $\gamma_{\boldsymbol{z}}^{\boldsymbol{RESP}}$ vs. higher values in $\gamma_{\boldsymbol{x}}^{\boldsymbol{RESP}}$ between 3 h and 4 h and high values of $\gamma_{\boldsymbol{z}}^{\boldsymbol{RESP}}$ vs. low values $\gamma_{\boldsymbol{x}}^{\boldsymbol{RESP}}$ between 4 h and 5 h) could indicate rearrangement of the arm or wrist during this period. The hypnogram for this subject with hypersomnolence is shown in (c). (d-e) For the second subject, the quality of the pulse wave reconstruction $\gamma_{\boldsymbol{y}}^{\boldsymbol{PW}}$ (orange) is very good for almost the entire night, while the respiratory reconstruction $\gamma_{\boldsymbol{\theta}}^{\boldsymbol{RESP}}$ yields only low PSI values. Panel (e) shows the hypnogram for this subject with a circadian rhythm sleep-wake disorder.

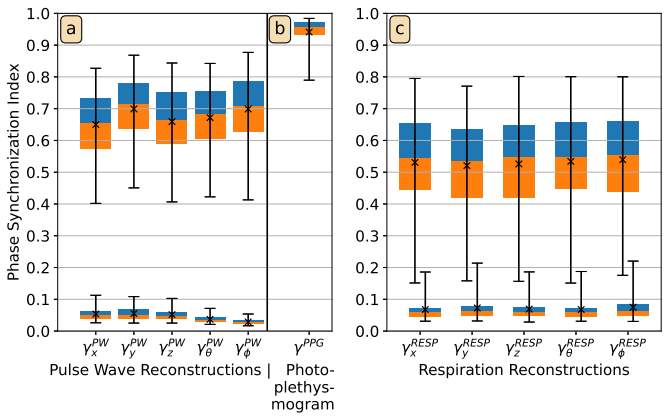

Fig. 3. **Box plots of phase synchronization indices** between acceleration-based reconstructions and ECG signal or respiration signal averaged across subjects. Results for pulse wave reconstructions and respiratory reconstructions are shown in (a) and (c), respectively. For each reconstruction, the orange part represents the values between the lower quartile and the median, and the blue part represents the values between median and upper quartile. Whiskers mark the 2.5% and the 97.5% quantile of the distributions among the 226 subjects. The average values appear as black crosses within the box plot. Box plots on the bottom of the figure summarize the results of the surrogate analysis utilizing time inverted data (see Section II-F). In addition, the results for optimally synchronized pulse wave data based on the PPG are shown in (b). In general, pulse wave reconstructions yield up to 20% higher PSI values than respiratory reconstructions, and $\boldsymbol{A}_{\boldsymbol{y}}^{\boldsymbol{PW}}$ and $\boldsymbol{A}_{\boldsymbol{\theta}}^{\boldsymbol{RESP}}$ perform slightly better than other signals to reconstruct pulse wave and respiration signal, respectively.

There seems to be no obvious relationship between reconstruction quality and sleep stages throughout the night as indicated by the hypnograms in panels Fig. 2 (c) and (e) for each subject. However, as expected, PSI values are dropping during wake episodes, see e.g. Fig. 2 (a) and (b) at times 3.9 h and 5.6 h. Furthermore, arm placement seems to be more important for respiration detection via wrist acceleration then for pulse wave detection.

Fig. 3 summarizes the PSI results for all 226 subjects. Averaging over all 30 second epochs during the night, an average PSI value has been calculated for each subject and each type of reconstruction. The box plots show mean, median, quartiles and 2.5 percent whiskers for the corresponding distributions of 226 PSI values in each case. One can see in Fig. 3 (a) that γ_y^{PW} and γ_ϕ^{PW} yield a slightly better synchronization with the ECG-derived instantaneous phase (mean values ≈ 0.70) as compared to γ_x^{PW}, γ_z^{PW}, and γ_θ^{PW} (mean values ≈ 0.67). The whiskers typically range from PSI values of 0.42 for the subjects with worst reconstruction quality to 0.85 for the subjects with best reconstruction quality. Regarding respiratory reconstructions, Fig. 3 (c) shows that most PSI values are in the range of 0.5 to 0.6. Here, the results derived from the wrist rotation angles are slightly better.

We note that the existence of different superior channels, i.e., y axis for pulse wave and rotation angle θ for respiration reconstruction is not surprising. While pulse waves crossing the wrist cause small internal wrist vibrations that are most pronounced perpendicular to the axis of wave propagation, respiration leads to changes of wrist orientation (i.e., wrist rotation). In fact, respiratory activity causes wrist movements only 'externally' via the arm or due to wrist placement next to the upper body. In this sense, it becomes clear why the quality of respiratory reconstructions is more variable throughout the night (Fig. 2) and their overall PSI values are lower than for pulse wave reconstructions.

In order to probe the significance of the PSI values calculated for pulse wave and respiratory reconstructions, Fig. 3 also includes PSI values for unsynchronized data (inverted time direction) and optimally synchronized pulse wave data using the PPG (see Section II-F for details). The corresponding box plots indicate that 97.5 percent of the 30-second epochs of surrogate data yield PSI values below 0.11 for pulse waves (Fig. 3 (a)) and 0.21 for respiration (Fig. 3 (c)). In contrast, optimally synchronized pulse waves derived from the PPG yield an average PSI value of 0.94 ± 0.06 (Fig. 3 (b)).

B. Sleep-Stage Dependent Synchronization

As shown in Fig. 2, the quality of pulse wave and respiration reconstructions may drop during nocturnal arousals and brief awakenings due to changes in neuronal characteristics [46]. To investigate systematically the reliability of our pulse wave and respiration reconstructions throughout the night, we calculate PSI values separately for each sleep stage taking into account all 226 subjects. Sleep stages based on 30-second epochs have been determined from the PSG data by trained experts following standard guidelines [11] to distinguish light sleep (stages N1 and N2), deep sleep (stage N3), and rapid eye movement (REM) sleep. As example, we choose γ_y^{PW} and γ_θ^{RESP} obtained from the pulse wave and respiration reconstruction,

TABLE I

AVERAGE PULSE WAVE AND RESPIRATION PHASE SYNCHRONIZATION INDICES SORTED BY RECONSTRUCTION SIGNAL AND SLEEP STAGE

	γ_x^{PW}	γ_y^{PW}	γ_z^{PW}	γ_θ^{PW}	γ_ϕ^{PW}	γ_x^{RESP}	γ_y^{RESP}	γ_z^{RESP}	γ_θ^{RESP}	γ_ϕ^{RESP}	# of epochs
all	0,65	0.70	0.66	0.67	0.70	0.53	0.52	0.53	0.54	0.54	189,635
Wake	0.50	0.53	0.50	0.52	0.54	0.40	0.38	0.39	0.40	0.38	25,849
REM	0.67	0.72	0.67	0.69	0.71	0.49	0.49	0.50	0.49	0.51	28,491
N1	0.63	0.69	0.64	0.66	0.68	0.48	0.46	0.47	0.48	0.48	31,653
N2	0.68	0.74	0.70	0.70	0.74	0.57	0.56	0.56	0.58	0.58	72,637
N3	0.72	0.76	0.73	0.74	0.77	0.65	0.64	0.65	0.66	0.67	31,005

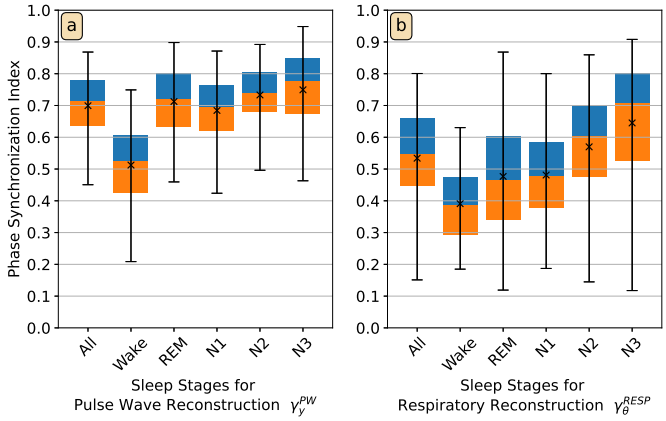

Fig. 4. **Box plots of phase synchronization indices during different sleep stages** for pulse waves, here $\gamma_{\boldsymbol{y}}^{\boldsymbol{PW}}$ in panel (a), and respiration, here $\gamma_{\boldsymbol{\theta}}^{\boldsymbol{RESP}}$ in (b). Average values for each subject were considered to obtain the box plots. The orange part of each box represents the values between the lower quartile and the median, and the blue part represents the values between the median and the upper quartile. The ends of the whiskers mark the 2.5% quantile and the 97.5% quantile, respectively. The total average values appear as black crosses in the box plot. For both reconstructions, best results are obtained for N2 and N3 sleep, whereas during wake, reconstruction quality is rather low.

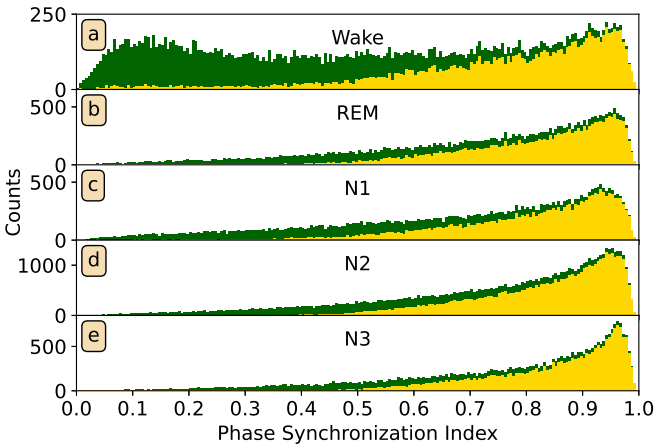

Fig. 5. **Histograms for PSI values of pulse wave reconstruction $\gamma_{\boldsymbol{y}}^{\boldsymbol{PW}}$ classified by sleep stages** showing the values for all epochs (green) and after internal evaluation and optimization of the pulse wave reconstruction procedure with a threshold of $\boldsymbol{\Gamma_{y,z}^{PW} > 0.5}$ (yellow). The results indicate that pulse wave reconstruction from accelerometer signals is much less reliable during consolidated wakefulness and that an internal evaluation and optimization procedure needs to be applied.

respectively and depict results in Fig. 4, see also [22]. The results for all pulse wave and respiration reconstructions for each sleep stage are listed in Table I.

Overall, our results (Table I, Fig. 4) indicate that particularly large PSI values are obtained for both pulse wave and respiration reconstruction during deep sleep N3 followed by light sleep stage N2, while lowest reliability is achieved during wakefulness. For REM sleep, pulse waves can be reconstructed very well (comparable to non-REM sleep), however, respiration reconstructions resemble the real respiratory signal to much lower degree. Again, this can be explained by the different nature of the reconstructions' origins – 'internal' pulse wave vibrations vs. 'external' respiration triggered wrist rotation. A lower reliability is also observed for the respiration reconstruction during N1 sleep with comparable values as for wakefulness and REM sleep. No particular advantage of certain axes or angles can be observed for any sleep stage (Table I). Fig. 4 also shows that the inter-quartile range is generally larger for respiration reconstructions, in particular during REM and N3 sleep. Although the averages of γ_θ^{RESP} are larger during N2 and N3, there are still outliers with nearly unsynchronized reconstruction ($\gamma_\theta^{RESP} < 0.2$). In contrast, for the pulse wave reconstructions, such outliers occur to much lower extent.

To illustrate the full distributions of the PSI values for the pulse wave reconstruction, Fig. 5 shows the histograms of all γ_y^{PW} values (for each epoch) during the different sleep stages. All histograms are peaked at PSI values close to 1, except for the one referring to wakefulness. In this case, another broad peak with very low PSI values indicates that pulse wave reconstructions are unreliable for about half of the 30-second epochs during wakefulness, most probably because of motion artifacts that disturb the wrist accelerometer signal during (consolidated) wakefulness but not during brief arousals. This is consistent with the recent observation that longer arousals and consolidated wakefulness lead to higher activity levels [46].

Therefore, our results suggest that the proposed approach of pulse wave (as well as respiration) reconstruction from accelerometer signals is applicable only during sleep and sedentary behaviour without significant wrist motion.

C. Effects of Sleep-Disordered Breathing on the Performance of Pulse Wave and Respiratory Signal Reconstruction

Sleep-related breathing disorders and in particular sleep apnea affect blood pressure regulation and lead to hypertension [47] and associated changes in pulse wave amplitude [48]. Therefore, it is reasonable to test the performance of pulse

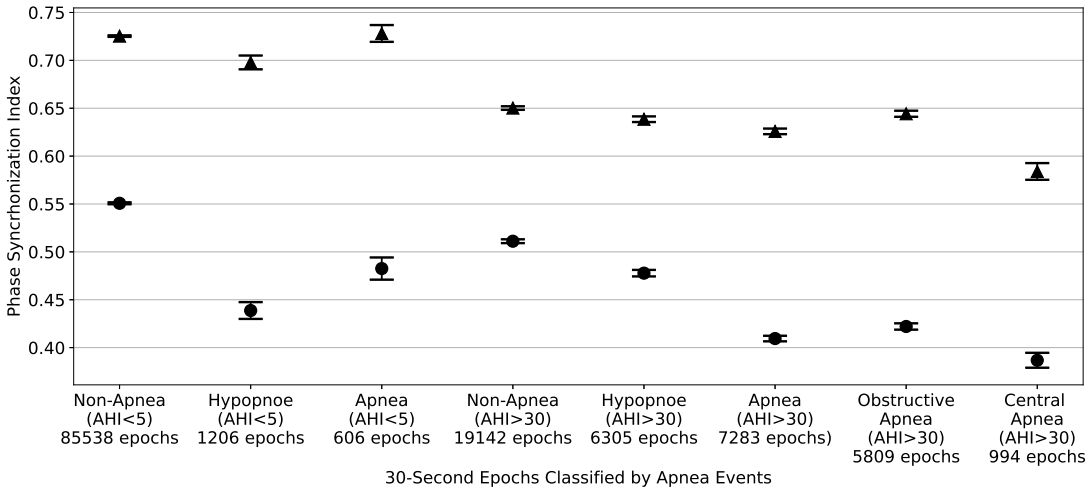

Fig. 6. **Effects of sleep-related breathing disorders** on the PSI for the pulse wave reconstruction γ_y^{PW} (▲) and the respiration reconstruction γ_θ^{RESP} (●) for subjects with low apnea hypopnea index (AHI) (<5 events/h) and high AHI (>30 events/h) averaged over all corresponding epochs (i) without apnea, (ii) with hypopnea, and (iii) with full apnea. For subjects with high AHI, PSI values for central and obstructive apnea are also reported separately. Error bars indicate the standard error. The labels include the number of epochs used for the corresponding averages. PSI values are highest for the γ_y^{PW} reconstruction for subjects with low AHI and about 10-15% lower for high AHI subjects. Interestingly, pulse wave reconstruction reliability for high AHI subjects seems to decline only slightly when hypopnea and apnea epochs are analyzed; for central sleep apnea this decline is most pronounced. For γ_θ^{RESP}, values are consistently much lower than for γ_y^{PW}. As expected γ_θ^{RESP} shows a stronger decline when apnea epochs are analyzed. However, for obstructive apnea, γ_θ^{RESP} is only slightly better as compared to central sleep apnea.

wave reconstruction from accelerometer signals under the condition of sleep apnea and to compare results to the obvious effect of sleep apnea on respiratory signal reconstruction. Fig. 6 shows that the largest pulse wave reconstruction PSI values γ_y^{PW} are obtained for healthy subjects with less than 5 apnea or hypopnea events per hour (i.e., AHI < 5). The same holds for the respiratory reconstruction γ_θ^{RESP}, however a drop in respiration reconstruction quality but not in pulse wave reconstruction quality is seen during the rare apneas and hypopneas in these subjects. The quality of both reconstructions is clearly reduced in subjects with more than 30 apnea or hypopnea events per hour, i.e., subjects suffering from severe sleep apnea. Again a further drastic decrease of γ_θ^{RESP} is seen during the actual apneas (but not hypopneas) in these patients, while this decrease is only marginal for γ_y^{PW}. When differentiating between obstructive apneas (caused by obstruction of the upper airways) and central apneas (due to absent respiratory drive from the brain stem), a slightly better reconstruction quality can be seen for the obstructive apneas, where the respiratory drive still persists.

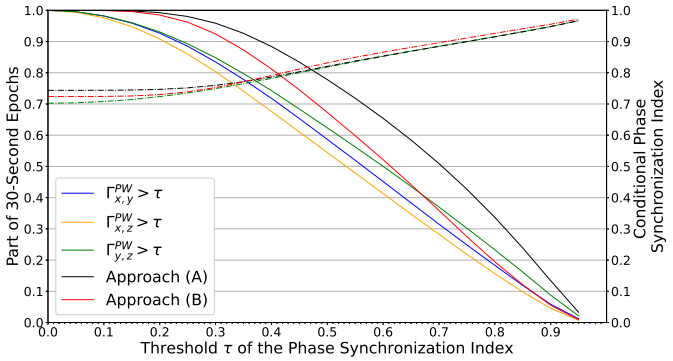

Fig. 7. **Performance of internal evaluation for increasing the quality of pulse wave reconstructions**. Inter-reconstruction phase synchronization indices $\mathbf{\Gamma_{i,j}^{PW}}$ were analyzed to identify 30-seconds epochs with reliable pulse wave reconstructions. Solid curves indicate the fraction of reliable 30-seconds epochs versus the inter-reconstruction PSI threshold $\boldsymbol{\tau}$, solid blue curve for $\mathbf{\Gamma_{x,y}^{PW}}$, green for $\mathbf{\Gamma_{y,z}^{PW}}$, and orange for $\mathbf{\Gamma_{x,z}^{PW}}$. Furthermore, to increase the fraction of reliable epochs and the reconstruction quality we introduced two approaches combining all three reconstructions: (A) – solid black curve and (B) – solid red curve. Dash-dotted curves show the average PSIs $\boldsymbol{\gamma_y^{PW}}$ (green), $\boldsymbol{\gamma_{(A)}^{PW}}$ (black), and $\boldsymbol{\gamma_{(B)}^{PW}}$ (red) between the selected reconstructions and our reference (ECG), calculated using only the reliable epochs. For example, the green dash-dotted curve shows $\boldsymbol{\gamma_y^{PW}}$ based on reliable epochs selected according to $\mathbf{\Gamma_{y,z}^{PW}} > \boldsymbol{\tau}$.

D. Identification of Reliable Epochs for the Reconstructed Signals

Checking the consistency (similarity) of pairs of reconstructed signals can be used as internal evaluation to identify 30-second epochs with a particularly reliable reconstruction. For this purpose, we have calculated the PSIs between pairs of independently derived reconstructed signals for each epoch. Then we selected time epochs with sufficient reconstruction quality by analyzing the PSI between two reconstructions. This approach represents an internal evaluation, which does not require recordings of ECG, PPG or respiratory flow. More specifically, we have calculated, e. g., the inter-reconstruction PSI $\Gamma_{x,y}^{PW}$ according to (1) for the two reconstructed phases φ_x^{PW} and φ_y^{PW} (instead of φ^{ECG}). Then, we have taken only those 30-second epochs into account, where $\Gamma_{x,y}^{PW}$ is above a certain threshold τ, indicating good synchronization between the reconstructions A_x^{PW} and A_y^{PW}. This internal evaluation approach leads to gaps in the reconstructed time series but, on the other hand, yields a much higher quality by only using

reliable epochs.

Fig. 7 (solid curves) shows how the fraction of usable 30-second epochs decreases as the threshold τ for the inter-reconstruction PSIs $\Gamma_{i,j}^{PW}$ is increased. Simultaneously, the average quality of the remaining reconstructed signals becomes higher as indicated by the increasing conditional averages of γ_j^{PW} (dash-dotted curves in Fig. 7).

For example, for reconstruction A_y^{PW} the internal evaluation yields an average $\gamma_y^{PW} = 0.81$ if $\Gamma_{y,z}^{PW} > 0.5$ is used for epoch selection (solid green curve in Fig. 7). In this case, the reconstruction is available for 62 percent of all epochs. Hence, if a pulse wave reconstruction for nearly two thirds of all epochs during the night is sufficient in a particular application, this simple internal evaluation procedure can be used to increase the average reconstruction quality indicator from 0.70 to 0.81 (green dash-dotted curve in Fig. 7 at τ = 0.5). Fig. 5 includes the histograms for the internally evaluated data with the threshold $\Gamma_{y,z}^{PW} > 0.5$ shown in yellow. One can see that the improvement is particularly effective for epochs of wakefulness, where most epochs with low reconstruction reliability (low γ_y^{PW}) are correctly identified and disregarded by the internal evaluation.

An additional improvement can be achieved by combinations of all three axes' data. Here, we developed two approaches for pulse wave reconstruction and one for respiration reconstruction:

Approach (A) Use A_x^{PW} if $\Gamma_{x,z}^{PW}$ exceeds $\Gamma_{x,y}^{PW}$, $\Gamma_{y,z}^{PW}$ and the threshold τ, or else use A_y^{PW} if $\Gamma_{x,z}^{PW}$ or $\Gamma_{y,z}^{PW}$ exceed τ. The results are shown as black curves in Fig. 7.

Approach (B) Use A_x^{PW} if $(\Gamma_{x,y}^{PW} + \Gamma_{x,y}^{PW})/2 > \tau$, or else use A_y^{PW} if $(\Gamma_{x,y}^{PW} + \Gamma_{y,z}^{PW})/2 > \tau$, or else use A_z^{PW} if $(\Gamma_{x,z}^{PW} + \Gamma_{y,z}^{PW})/2 > \tau$. The results are shown as red curves in Fig. 7.

Approach (C) Use A_ϕ^{RESP} if $\Gamma_{y,z}^{RESP}$ exceeds $\Gamma_{x,y}^{RESP}$, $\Gamma_{x,z}^{RESP}$ and the threshold τ, or else use A_θ^{RESP} if $\Gamma_{x,y}^{RESP}$ or $\Gamma_{x,z}^{RESP}$ exceed τ.

For both approaches (A) and (B) the number of 30-second epochs decreases slower with increasing threshold, see Fig. 7. For half of all 30-second epochs a PSI of 0.88 can be achieved with approach (A) and 0.87 with approach (B). These results correspond to a nearly perfect pulse wave reconstruction in the considered epochs, since they are very close to the average PSI for the PPG ($\gamma^{PPG} = 0.94$, see Fig. 4).

Fig. 8 shows our results for reconstructions optimized by internal evaluation considering only 50% of all epochs. The selection of particularly good epochs leads to generally much larger PSI values than those reported in Fig. 4 for all epochs. The improvement is much larger for the pulse wave reconstructions than for the respiratory reconstructions, however, the general sleep-stage stratification pattern as observed in Fig. 4 is preserved in both cases.

IV. Discussion

We have conducted a systematic comparison between PSG-recorded cardiac dynamics and respiratory activity and

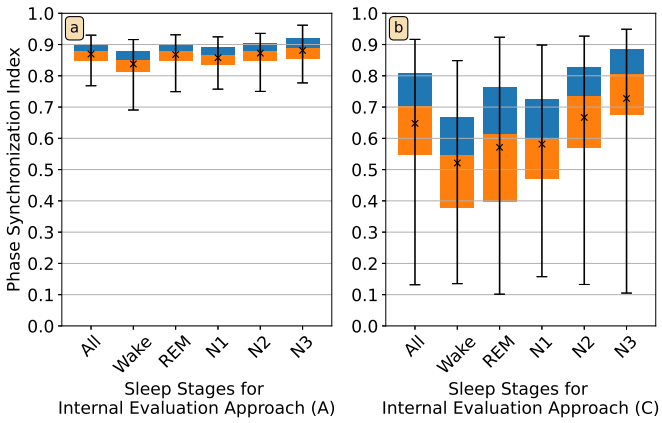

Fig. 8. **Internal Evaluation Effect on Sleep Stages**. Same as Fig. 4, but for signals optimized by internal evaluation with signal selection according to approach (A) and (C) (see text); 50% of all epochs are used. The inter-reconstruction PSI threshold τ is 0.7 for the pulse wave reconstructions and 0.92 for the respiration reconstructions.

corresponding signal reconstructions as derived from high-resolution wrist accelerometer data. We show that all reconstructions obtained from the accelerometer's axes and angles perform similarly well for both, pulse wave and respiration reconstruction. The overall synchronization between reconstructed signal and PSG signal is higher for the pulse waves with an average of $\gamma^{PW} \approx 0.68$ as compared to $\gamma^{RESP} \approx 0.53$ for respiration. This may be because of the different underlying phenomena giving rise to the reconstructed signals. While the 'external' respiration-triggered wrist rotations could be sensitive to different placements of the arm, the 'internal' pulse wave vibrations caused by the pulsatile blood flow in the wrist seem to be less affected by arm positioning.

Such interpretation could explain the stronger sleep-stage dependence we observe for the respiration reconstructions, where muscle atonia during REM sleep can diminish respiratory-triggered wrist movements. Overall, we obtain for the respiration reconstructions an average of $\gamma^{RESP} \approx 0.50$ for REM and $\gamma^{RESP} \approx 0.61$ for N2-N3 non-REM sleep. In contrast, average values for the pulse wave reconstructions are much higher with averages $\gamma^{PW} \approx 0.69$ and $\gamma^{PW} \approx 0.73$ for REM and N2-N3 non-REM sleep, respectively. Our analyses also show that pulse wave and respiration reconstruction from accelerometer data does not work as well during wakefulness, perhaps because of frequent body movements that are characteristic for this stage. Surprisingly, however, we find that pulse wave reconstructions are hardly affected by sleep apnea epochs per se. The reduced overall quality that we observe in patients with severe sleep apnea (during normal breathing as well as during apnea epochs) could therefore be related to a more restless and shallow sleep that typically occurs in these patients.

Compared with seismocardiography and ballistocardiography (see Section II.B), our suggested approach using wrist accelerometers has advantages for a screening of larger population groups and general population-based cohort studies, since the sensor is worn like a normal wrist watch and can

thus be handed to each subjects in the study center with very brief instructions. No preparation of a bed or chair at the home of the subject, no data transmission infrastructure and no visits of care personal to the home are needed. The sensor can easily be returned to the study center by postal mail, after the pre-programmed recording period has ended. Ballistocardiography, on the other hand, has advantages for monitoring specific subjects for a long time, in particular disabled or elderly persons or children, since this method requires less compliance of the subjects but more effort from the study center or hospital.

Our proposed approach for simultaneously reconstructing pulse wave and respiration signals from wrist accelerometers has advantages and disadvantages compared to wrist or finger photoplethysmography (PPG). Certainly, pulse waves are more directly assessed by PPG. Our results show that if one has to rely on wrist actigraphy only, reliable pulse waves can only be reconstructed for parts of the night and particularly not for periods of nocturnal wakefulness. However, the reconstruction of breathing activity from a PPG is much more indirect – a double reconstruction is involved, since one must first obtain the timing of the heartbeats from the plethysmogram, and then breathing activity has to be derived based on heart rate modulations via respiratory sinus arrhythmia (RSA). In addition, respiration can also affect pulse transition times, so that the first reconstruction step becomes less reliable. Furthermore, RSA is typically weaker in elderly subjects, so that the reliability of the second reconstruction step will become age dependent and probably also be affected by cardio-respiratory impairments. In our previous work [22], we have shown that the reconstruction of breathing activity from the timing of the R peaks in the ECG is less reliable than reconstruction from wrist accelerometry. Therefore, we are convinced that PPG approaches cannot yield sufficient quality of reconstructed respiration data in large general population-based studies.

A possible next step of our research should study the relationship between the two signals reconstructed from the same wrist accelerometer. In this context, the overall question would be whether the reconstructed pulse waves and respiratory activities are sufficiently reliable so that different aspects of cardio-respiratory coupling [49]–[51] can be derived from them. Additionally, one could probe, e.g., the dependence of cardio-respiratory coupling on sleep stages (using data such as those studied here) or derive cardio-respiratory coupling in large population-based cohort studies with many thousands of participants (see below). To test how reliable different aspects of cardio-respiratory coupling can be derived from the reconstructed data, several measures of cardio-respiratory synchronization [52], [53] and cardio-respiratory coordination [44] shall be applied to the reconstructed data and the reference PSG data.

V. Conclusion

Our paper introduces a novel approach for simultaneously obtaining time series of cardiac and respiratory dynamics during sleep. Unlike most previous approaches, the presented methodology relies entirely on a single wrist accelerometer, which is often used in large cohort studies, e.g., the German National Cohort study [54] with ≈25,000 SOMNOwatch™ recordings up to now. Another example is the UK Biobank study, in which wrist-worn accelerometers were used to assess physical activity in 100,000 volunteers [55]. Large population-based studies often include actigraphy (accelerometry) as the only continuously measured physiological signal because it can be easily recorded by a smart watch and does not require electrodes, flow sensors, or chest belts.

Our proposed phase synchronization metric evaluates the timing of pulse waves and respiratory cycles and is independent of amplitude changes. This is adequate for our signal reconstructions since changes in wrist position with respect to the body as well as changes in the position of the device at the wrist influence the signal amplitude. Therefore, our approach may not be used for a reliable derivation of stroke or breath volume variations. Furthermore, the approach works only if no other (i.e., voluntary) movements occur and thus, is limited to the sleep period. This is consistent with our finding that the best reconstruction quality is achieved during deep sleep, followed by light sleep N2 and REM sleep, and at last nocturnal wakefulness. Nevertheless, pulse wave reconstructions are just weakly affected by apnea and hypopnea events, and their reliability can be increased by internal evaluation if the reconstructed signals are not needed for the entire sleep duration. Ultimately, our approach could be used to monitor pulse wave characteristics during sleep in combination with or as a substitute of a wrist or finger photoplethysmogram.

Acknowledgment

We thank Antonia Graf, Maria Kluge, and Luise Pelikan (Charité - Universitätsmedizin Berlin) for data acquisition in the sleep laboratories. We also thank Alexander Müller (Technical University of Munich) for providing R-peak detection in SOMNOwatch™ data and Yaopeng Ma (Bar-Ilan University, Ramat Gan) for discussion and data synchronization.

References

[1] H. R. Colten and B. M. Altevogt, Eds., *Sleep Disorders and Sleep Deprivation: An Unmet Public Health Problem*, Washington (DC), 2006.
[2] D. R. Gold *et al.*, "Rotating shift work, sleep, and accidents related to sleepiness in hospital nurses," *American journal of public health*, vol. 82, no. 7, pp. 1011–1014, 1992.
[3] L. K. Barger *et al.*, "Extended work shifts and the risk of motor vehicle crashes among interns," *The New England journal of medicine*, vol. 352, no. 2, pp. 125–134, 2005.
[4] A. N. Vgontzas *et al.*, "Adverse effects of modest sleep restriction on sleepiness, performance, and inflammatory cytokines," *The Journal of clinical endocrinology and metabolism*, vol. 89, no. 5, pp. 2119–2126, 2004.
[5] L. K. Barger *et al.*, "Impact of extended-duration shifts on medical errors, adverse events, and attentional failures," *PLoS medicine*, vol. 3, no. 12, p. e487, 2006.
[6] A. B. Newman *et al.*, "Daytime sleepiness predicts mortality and cardiovascular disease in older adults. the cardiovascular health study research group," *Journal of the American Geriatrics Society*, vol. 48, no. 2, pp. 115–123, 2000.
[7] H. K. Yaggi *et al.*, "Obstructive sleep apnea as a risk factor for stroke and death," *The New England journal of medicine*, vol. 353, no. 19, pp. 2034–2041, 2005.
[8] N. Covassin and P. Singh, "Sleep duration and cardiovascular disease risk: Epidemiologic and experimental evidence," *Sleep medicine clinics*, vol. 11, no. 1, pp. 81–89, 2016.

[9] M. Zinkhan and J. W. Kantelhardt, "Sleep assessment in large cohort studies with high-resolution accelerometers," *Sleep medicine clinics*, vol. 11, no. 4, pp. 469–488, 2016.

[10] A. Rechtschaffen and A. Kales, *A manual of standardized terminology, techniques and scoring system for sleep stages of human subjects. Allan Rechtschaffen and Anthony Kales, editors*, ser. NIH publication no. 204. Bethesda, Md.: U. S. National Institute of Neurological Diseases and Blindness, Neurological Information Network, 1968.

[11] R. B. Berry *et al.*, "The AASM manual for the scoring of sleep and associated events: rules, terminology and technical specifications, version 2.5." *American Academy of Sleep Medicine, Darien, IL*, 2018.

[12] J.-H. Byun *et al.*, "The first night effect during polysomnography, and patients' estimates of sleep quality," *Psychiatry research*, vol. 274, pp. 27–29, 2019.

[13] B. W. Riedel *et al.*, "First night effect and reverse first night effect in older adults with primary insomnia: does anxiety play a role?" *Sleep Medicine*, vol. 2, no. 2, pp. 125–133, 2001.

[14] G. Curcio *et al.*, "Paradoxes of the first-night effect: a quantitative analysis of antero-posterior EEG topography," *Clinical neurophysiology*, vol. 115, no. 5, pp. 1178–1188, 2004.

[15] D. J. Kupfer *et al.*, "Psychomotor activity in affective states," *Archives of general psychiatry*, vol. 30, no. 6, pp. 765–768, 1974.

[16] T. R. Colburn *et al.*, "An ambulatory activity monitor with solid state memory," *ISA transactions*, vol. 15, no. 2, pp. 149–154, 1976.

[17] S. Ancoli-Israel *et al.*, "The role of actigraphy in the study of sleep and circadian rhythms," *Sleep*, vol. 26, no. 3, pp. 342–392, 2003.

[18] C. McCall and W. V. McCall, "Objective vs. subjective measurements of sleep in depressed insomniacs: first night effect or reverse first night effect?" *Journal of clinical sleep medicine*, vol. 8, no. 1, pp. 59–65, 2012.

[19] A. Godfrey *et al.*, "Direct measurement of human movement by accelerometry," *Medical engineering & physics*, vol. 30, no. 10, pp. 1364–1386, 2008.

[20] A. Sadeh *et al.*, "The role of actigraphy in the evaluation of sleep disorders," *Sleep*, vol. 18, no. 4, pp. 288–302, 1995.

[21] J. Zschocke *et al.*, "Detection and analysis of pulse waves during sleep via wrist-worn actigraphy," *PloS one*, vol. 14, no. 12, p. e0226843, 2019.

[22] J. Leube *et al.*, "Reconstruction of the respiratory signal through ECG and wrist accelerometer data," *Scientific reports*, vol. 10, no. 1, p. 14530, 2020.

[23] J. M. Zanetti and D. M. Salerno, "Seismocardiography: a technique for recording precordial acceleration," in *Computer-based medical systems*, I. N. Bankman and J. E. Tsitlik, Eds. Los Alamitos, CA: IEEE Computer Society Press, 1991, pp. 4–9.

[24] O. T. Inan *et al.*, "Ballistocardiography and seismocardiography: a review of recent advances," *IEEE Journal of Biomedical and Health Informatics*, vol. 19, no. 4, pp. 1414–1427, 2015.

[25] M. Jafari Tadi *et al.*, "A real-time approach for heart rate monitoring using a Hilbert transform in seismocardiograms," *Physiological Measurement*, vol. 37, no. 11, pp. 1885–1909, 2016.

[26] K. Pandia *et al.*, "Extracting respiratory information from seismocardiogram signals acquired on the chest using a miniature accelerometer," *Physiological Measurement*, vol. 33, no. 10, pp. 1643–1660, 2012.

[27] M. Jafari Tadi *et al.*, "Accelerometer-based method for extracting respiratory and cardiac gating information for dual gating during nuclear medicine imaging," *International Journal of Biomedical Imaging*, vol. 2014, p. 690124, 2014.

[28] P. Castiglioni *et al.*, *2007 Annual International Conference of the IEEE Engineering in Medicine and Biology Society*. Piscataway, NJ: IEEE Service Center, 2007.

[29] A. Albukhari *et al.*, "Bed-embedded heart and respiration rates detection by longitudinal ballistocardiography and pattern recognition," *Sensors*, vol. 19, p. 1451, 2019.

[30] C. Carlson *et al.*, "Bed-based ballistocardiography: Dataset and ability to track cardiovascular parameters," *Sensors*, vol. 21, p. 156, 2021.

[31] A. Ullal *et al.*, "Non-invasive monitoring of vital signs for older adults using recliner chair," *Health and Technology*, vol. 11, pp. 169–184, 2021.

[32] G. Wusk and H. Gabler, "Non-invasive detection of respiration and heart rate with a vehicle seat sensor," *Sensors*, vol. 18, p. 1463, 2018.

[33] H. Liu *et al.*, "Recent development of respiratory rate measurement technologies," *Physiological Measurement*, vol. 40, p. 07TR01, 2019.

[34] C. Massaroni *et al.*, "Contact-based methods for measuring respiratory rate," *Sensors*, vol. 19, p. 908, 02 2019.

[35] J. Hernandez *et al.*, "Biowatch: Estimation of heart and breathing rates from wrist motions," in *Proceedings of the 9th International Conference on Pervasive Computing Technologies for Healthcare*, B. Arnrich *et al.*, Eds. ICST, 20.05.2015 - 23.05.2015.

[36] J. Hernandez *et al.*, "Wearable motion-based heart-rate at rest: A workplace evaluation," *IEEE Journal of Biomedical and Health Informatics*, vol. 23, pp. 1920–1927, 2019.

[37] M. Haescher *et al.*, "Seismotracker: Upgrade any smart wearable to enable a sensing of heart rate, respiration rate, and microvibrations," in *Proceedings of the 2016 CHI Conference Extended Abstracts on Human Factors in Computing Systems*, J. Kaye *et al.*, Eds. New York, USA: ACM Press, 2016, pp. 2209–2216.

[38] Y. Yao *et al.*, "Unobtrusive estimation of cardiovascular parameters with limb ballistocardiography," *Sensors*, vol. 19, p. 2922, 2019.

[39] D. Gabor, "Theory of communication. the analysis of information," *Journal of the Institution of Electrical Engineers-Part III: Radio and Communication Engineering*, vol. 93, no. 26, pp. 429–441, 1946.

[40] B. Boashash, "Estimating and interpreting the instantaneous frequency of a signal. i - fundamentals. ii - algorithms and applications," *Proceedings of the IEEE*, vol. 80, no. 4, pp. 540–568, 1992.

[41] M. Rosenblum *et al.*, "Chapter 9 - Phase synchronization: From theory to data analysis," in *Neuro-informatics and neural modelling*, ser. Handbook of Biological Physics, F. Moss, Ed. Elsevier, 2001, vol. 4, pp. 279–321.

[42] P. Wohlfahrt *et al.*, "Transitions in effective scaling behavior of accelerometric time series across sleep and wake," *EPL (Europhysics Letters)*, vol. 103, no. 6, p. 68002, 2013.

[43] R. Quian Quiroga *et al.*, "Event synchronization: A simple and fast method to measure synchronicity and time delay patterns," *Physical Review E*, vol. 66, no. 4, p. 041904, 2014.

[44] M. Riedl *et al.*, "Cardio-respiratory coordination increases during sleep apnea," *PLoS ONE*, vol. 9, no. 4, p. e93866, 2014.

[45] M. Rosenblum *et al.*, "Phase synchronization of chaotic oscillators," *Physical Review Letters*, vol. 76, no. 11, pp. 1804–1807, 1996.

[46] H. Dvir *et al.*, "A biased diffusion approach to sleep dynamics reveals neuronal characteristics," *Biophysical journal*, vol. 117, no. 5, pp. 987–997, 2019.

[47] R. P. Pedrosa *et al.*, "Obstructive sleep apnea: the most common secondary cause of hypertension associated with resistant hypertension," *Hypertension (Dallas, Tex. : 1979)*, vol. 58, no. 5, pp. 811–817, 2011.

[48] J. Haba-Rubio *et al.*, "Obstructive sleep apnea syndrome: effect of respiratory events and arousal on pulse wave amplitude measured by photoplethysmography in NREM sleep," *Sleep & breathing*, vol. 9, no. 2, pp. 73–81, 2005.

[49] R. Bartsch *et al.*, "Phase transitions in physiologic coupling," *Proc. Natl. Acad. Sci. USA*, vol. 109, pp. 10 181–10 186, 2012.

[50] H. Krause *et al.*, "On the difference of cardiorespiratory synchronisation and coordination," *Chaos*, vol. 27, no. 9, p. 093933, 2017.

[51] M. Elstad *et al.*, "Cardiorespiratory interactions in humans and animals: rhythms for life," *Am. J. Physiol. Heart Circ. Physiol.*, vol. 315, no. 1, pp. H6–H17, 2018.

[52] R. Bartsch *et al.*, "Experimental evidence for phase synchronization transitions in the human cardio respiratory system," *Physical Review Letters*, vol. 98, no. 2, p. 054102, 1998.

[53] A. Kuhnhold *et al.*, "Quantifying cardio-respiratory phase synchronization – a comparison of five methods using ECGs of post-infarction patients," *Physiological Measurement*, vol. 38, pp. 925–939, 2017.

[54] GNC Consortium, "German National Cohort: aims, study design and organization," *European Journal of Epidemiology*, vol. 29, no. 5, pp. 371–382, 2014.

[55] A. Doherty *et al.*, "Large scale population assessment of physical activity using wrist worn accelerometers: the UK Biobank study," *PLoS ONE*, vol. 12, no. 2, p. e0169649, 2017.